Supporting information

Insights on Hydrogen Bond assisted Solvent Selection in Certain Acid-Base Heterogeneous Catalysis through Acceptor and Donor Number

Vijaykumar S Marakatti, *[a] Jiří Klimeš,[b] Palraj Kasinathan,[a] Kesha Sorathia,[c] David P. Tew,[c] Eric M Gaigneaux[a]*

[a]Institute of Condensed Matter and Nanosciences (IMCN), MOlecular chemistry, Solids and caTalysis (MOST), Université catholique de Louvain (UCLouvain), Place Louis Pasteur, B-1348 Louvain-la-Neuve, Belgium.

[b] Department of Chemical Physics and Optics, Faculty of Mathematics and Physics, Charles University, Ke Karlovu 3, Prague 121 16, Czech Republic

[c]Physical and Theoretical Chemistry Laboratory, Oxford University, South Parks Road, Oxford OX1 3QZ, United Kingdom

**corresponding author: eric.gaigneaux@uclouvain.be, chmvijay@gmail.com*

Number of Pages - 24

Experimental details - Page 2-4

Number of Schemes - 4 (SchemeS1- SchemeS4)

Number of Tables - 4 (Table S1-TableS4)

Number of Figures - 12 (FigureS1-FigureS11)

1. Experimental Details

1.1. Materials:

All the zeolite samples H-Y (CBV-500), H-Beta (CP-814E) were obtained from zeolyst International, USA. The hydrotalcite (Mg/Al=3) catalyst was obtained from Sigma Aldrich, USA. Sulphated zirconia (SZ) and Zn-Beta catalysts were synthesized as reported in our earlier work.[1-3]

1.2. Characterization of catalyst

FT-IR spectra of the solid catalysts were taken in ATR mode using a spectrometer IFS55 Equinox (Bruker) equipped with a DTGS detector. The spectra recorded with 100 scans between 400 and 4000 cm^{-1} at a resolution of 4 cm^{-1}. The liquid samples (mixtures of two solvents) were analysed in the transmission mode by adding a drop of the sample between two KBr windows and spectra recorded with same parameters as solid samples. UV–vis spectra of resorcinol in different solvents collected on a Beckman Coulter DU800 spectrometer in absorption mode between 200 nm and 800 nm at a speed of 1200 nm/min. The sample was prepared by adding 2 mg of resorcinol in 20 ml of solvent. Before analysis of sample, blank measurements collected placing only solvent in the quartz cuvette. TGA curves were recorded simultaneously using Mettler Toledo TGA/SDTA851e instrument by heating the samples from 30 to 800 °C at the rate of 10 ˚C /min in flowing nitrogen gas (10ml/min).

1.3. Computational Details

The Gaussian 09-software program did geometry optimization, determination of interaction energy and bond length analyses. The geometry of the solvent-reactant was constructed in such a way that hydrogen bonding between the reactant and solvent molecules is possible through a solvent functional group (-Cl, NO_2, CN, SO, O, -OH, =C-H) keeping distance between them to minimum 3 Å. The density functional theory (DFT) have been carried out using B3LYP/6-31G (d,p) basis set. The B3LYP/6-31G (d,p) basis set is adequate to determine the solvent –reactant interactions due to their comparable vibrational frequencies obtained theoretically and by FTIR experimentally. Interaction energy for hydrogen-bonded complex (ΔE_{HB}) is calculated as the difference between the energy of hydrogen-bonded complex and the summation of the energy of each component as given below

$$\Delta E_{HB} = E_{complex} - \sum E_{componenet1} + E_{component2}$$

where $E_{complex}$ and E component are optimized energy of hydrogen bonded complex and each individual component monomer, respectively. The interaction energy was corrected from the basis set superposition error (BSSE) by virtue of counterpoise method.[4-5] The hydrogen-bonded complex is more stable if the interaction energy is more negative compared to the other hydrogen bonded configurations. Vibrational frequency was calculated using a 0.96 scaling factor. The optimized structure 4T zeolite model was used to compare the adsorption energies with the solvents using DFT method.[6] The 4T zeolite model was built using Si tetrahedral model from the Gaussian view and finally connecting them. Some Si atoms were replaced with Al atoms and then an additional acidic proton was used added to bridged oxygen.[6] The structure was initially relaxed without fixing the atoms, and later for adsorption study, we fixed all the atoms of zeolite except the acidic proton and solvent molecule. The dangling bonds in these clusters are saturated with H atoms. For adsorption study the solvent molecules were placed just above the 4T zeolite model at distance of 3 Å in such way that hydrogen bonding between the zeolite (acidic proton) and solvent functional group is possible through a (-Cl, NO_2, -CN, SO, O, -OH, =C-H).

The calculations for the periodic models of zeolites were performed using the Vienna *ab initio* simulations package (VASP).[7-9] The Perdew-Burke-Ernzerhof (PBE) exchange-correlation functional together with the "D3" dispersion correction of Grimme and co-workers was used.[10-11] For the D3 correction, damping was set to the Becke-Johnson type.[12] Geometry optimization used a (2×2×1) k-point grid and a plane-wave cut-off of 400 eV. The structure was optimized until the largest atomic force fell below 0.02~eV/\Å. The initial structure of pure silica zeolite was the BEA structure from zeolite structure database. Different Al sittings were tested and for the final calculations position adjacent to the large channel along the [100] direction was chosen.[13] For each molecule, we constructed an initial structure for optimization using a script that aligned the cluster model onto the periodic framework. The structure was additionally manually rotated in the cases where the molecule overlapped with the zeolite framework.

1.4. Catalytic Test

1.4.1. Friedel -Craft alkylation: In a typical procedure for resorcinol alkylation, resorcinol (20 mmol), tertiary butanol (40 mmol), HY zeolite (0.22 g) and solvent (2 ml) were added to a 100 ml glass reactor equipped with a reflux condenser and a magnetic stirrer. The required temperature for the reaction (80°C) was controlled and monitored by a PID temperature

controller and a thermometer, respectively. After periodic intervals of time, 10 µl of reaction mixture was diluted with methanol and analysed by gas chromatography (Shimadzu-2014, FID detector) using a RTX-5 column. The products were confirmed by injecting standard samples and NMR analysis as reported in previous work.[3, 14]

1.4.2. Butanol esterification: The esterification reactions were carried out in a 50 mL round-bottomed flask equipped with a reflux condenser. In a typical run, acetic acid (200 mmol), solvent (5 ml) and H-beta zeolite (0.4 g) were charged into the flask and heated to the reaction temperature (80 °C). When attaining the desired temperature, *n*-butanol (50 mmol) was introduced into the reaction mixture and this moment was considered as the zero-reaction time. Samples were collected at regular intervals and analysed by gas chromatography.[15]

1.4.3. Knoevenagel condensation: In a typical procedure, benzaldehyde (10 mmol), ethyl cyanoacetate (12 mmol), catalyst hydrotalcite (50 mg), solvent (3 ml) and 0.2 ml N, N-DMF (internal standard) were added to a 100 ml glass reactor equipped with a reflux condenser and a magnetic stirrer in an inert atmosphere. The required temperature for the reaction (80°C) was controlled and monitored by a PID temperature controller and thermometer, respectively. After periodic intervals of time, 20 ul µl of reaction mixture was diluted with methanol and analyzed by gas chromatography (Shimadzu-2014, FID detector) using a RTX-5 column. The products were confirmed by injecting standard samples during the analysis**.**

1.4.4. Claisen-Schmidt condensation: In a typical procedure, benzaldehyde (15 mmol), acetophenone (10 mmol), hydrotalcite (200 mg), solvent (3 ml) and 0.2 ml N, N-DMF (internal standard) were added to a 100 ml glass reactor equipped with a reflux condenser and a magnetic stirrer in an inert atmosphere at 140 °C. After periodic intervals of time, 20 µl of reaction mixture was diluted with methanol and analysed by gas chromatography (Shimadzu-2014, FID detector) using a RTX-5 column. The products were confirmed by injecting the standard compounds in GC.

1.4.5 Acylation of anisole: In a typical procedure, anisole (10 mmol), acetic anhydried (50 mmol), H-Beta zeolite (200 mg), solvent (3 ml) and 0.2 ml o-xylene (internal standard) were added to a 100 ml glass reactor equipped with a reflux condenser and a magnetic stirrer in an inert atmosphere. The required temperature for the reaction (80°C) was controlled and monitored by a PID temperature controller and thermometer, respectively. After regular intervals of time , 10 µl of reaction mixture was diluted with methanol and analyzed by gas

chromatography (Shimadzu-2014, FID detector) using a RTX-5 column. The products were confirmed by injecting pure 4-methoxy acetophenone in GC.

1.4.6. Prins reactions: Prins Cyclization and condensation reactions were performed as reported earlier in our studies.[1-2]

1.5. Solvent Adsorption study on zeolites: In this case, around 0.2 ml of solvent was dissolved in 5ml of TBA and to this solution, around 0.2 gram of H-Y zeolite was added and stirred at 80 °C for an hour followed by filtration and drying at room temperature overnight. The TGA measurements of so obtained catalysts were measured in N_2 atmosphere.

1.6. Solvent Adsorption study on hydrotalcite: In this case, around 0.2 ml of solvent was dissolved in 5ml of ethyl acetate and to this solution, around 0.2 gram of H-Y zeolite was added and stirred at 80 °C for an hour followed by filtration and drying at room temperature overnight. The TGA measurements of so obtained catalysts were measured in N_2 atmosphere.

Scheme.S1. Schematic representation of acid catalysed reactions a) Friedel-Craft alkylation b) n-butanol esterification c) Prins cyclization, and d) Prins condensation.

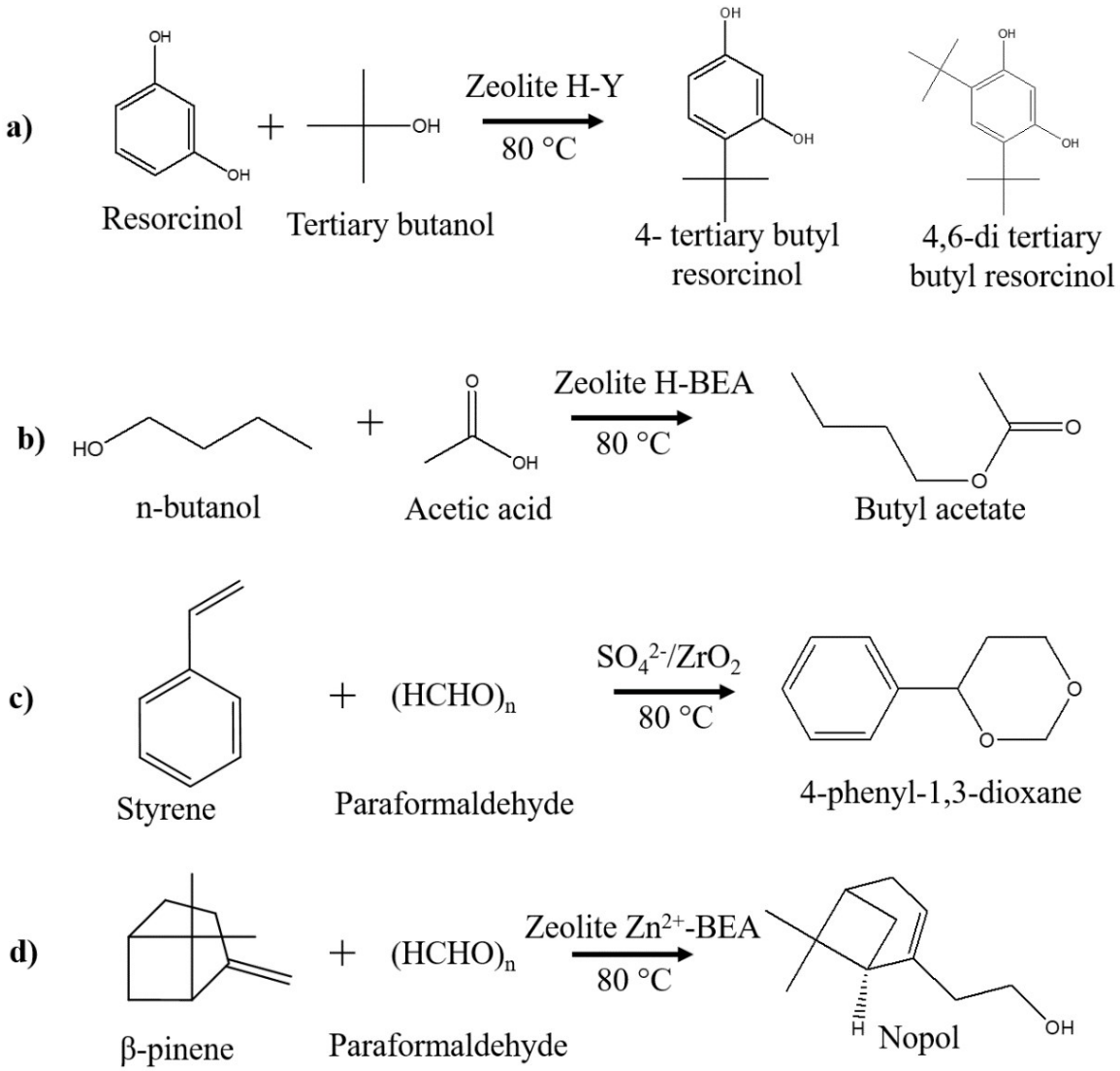

Scheme.S2. Schematic representation of base catalysed reaction a) Knoevenagel condensation, and b) Claisen-Schmidt Condensation.

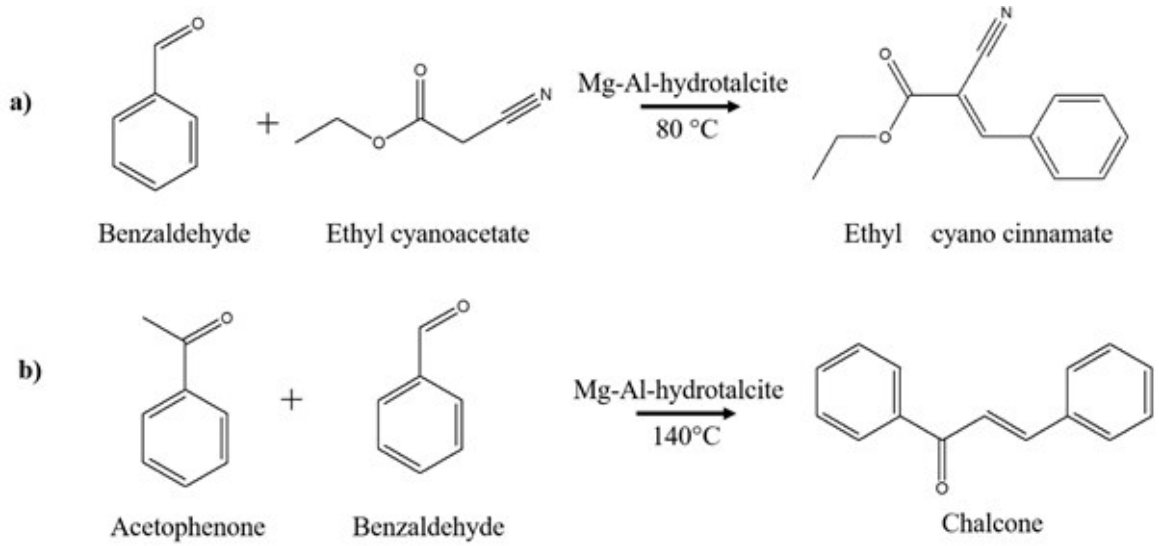

Scheme S3. Schematic depiction of the formation of carbocation and carbanion in a) acid, and b) base catalysed reactions**.**

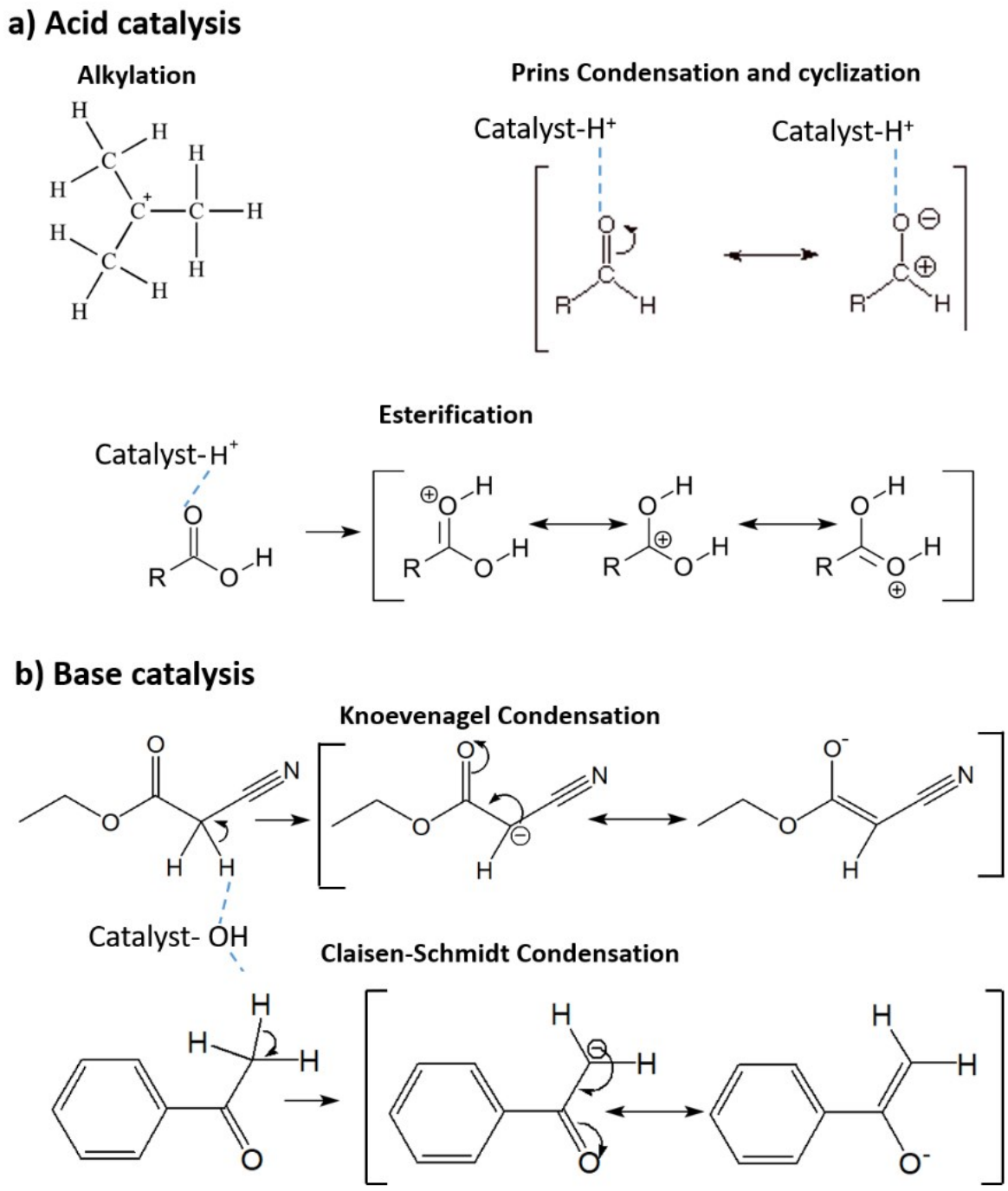

Scheme S4. Schematic representation of acid catalysed acylation of anisole over H-beta.

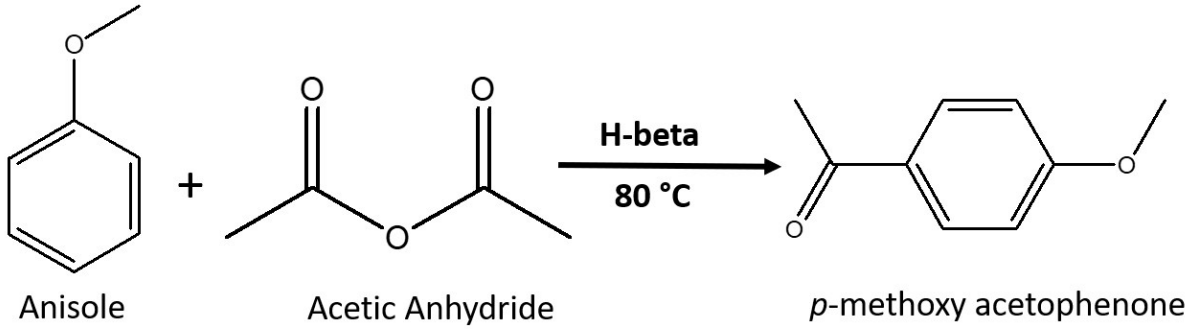

Table S1 Catalytic activity of resorcinol alkylation in different solvents.

Entry	Solvent	Conversion of Resorcinol	Selectivity for products		
			4-TBR	4,6-TBR	Others*
1	No Solvent	43.2	84.1	5.38	10.5
2	Tertiary butanol	37.3	82.5	5.56	11.9
3	Cyclohexane	44.8	83.8	3.2	13.0
4	Benzene	50.9	86.2	5.1	8.7
5	1,2-dicholoroethane	59.3	94	2.61	3.4
6	Nitrobenzene	42.2	82.7	5.3	12.0
7	Benzonitrile	35.8	66.4	3.8	29.8
8	Dioxane	30.5	80.5	3.1	16.4
9	DMSO	0	0	0	0
10	Isopropyl alcohol	22.8	87.2	5.2	7.6
11	n-butanol	33.0	86.3	4.6	9.1
12	Water	0	0	0	0

Reaction conditions: Resorcinol =20 mmol g, TBA = 40 mmol, Solvent = 2 ml, Temperature = 80 °C, *o*-Xylene = 0.9ml (internal standard), Reaction time= 14 h.

**Others mainly consist of 2-TBR and R-MTBE.

Table S2 Calculated bond distances ($d_{X\cdots H}$, Å), IR Vibrational Frequency (cm^{-1}) and interaction energy (ΔE_{HB}, kJ/mol) of hydrogen bond between the alcohols (resorcinol, tertiary butanol) and the solvents.

	Resorcinol			Tertiary butanol		
Solvent	$dx\cdots_H$	cm^{-1}	ΔE_{HB}	$d_{O\cdots H}$	cm^{-1}	ΔE_{HB}
Cyclohexane	2.76	3616	+1.25	2.75	3584	+2.1
Benzene	2.50	3553	-9.2	2.60	3564	-5.0
1,2 dichloroethane	2.56	3556	-9.6	2.78	3570	-10.4
Nitrobenzene	1.95	3533	-18.8	2.10	3548	-12.5
Benzonitrile	2.14	3523	-20.0	2.10	3539	-15.4
1,4-dioxane	1.82	3396	-27.2	1.93	3502	-15.9
Dimethyl sulfoxide	1.74	3189	-43.93	1.88	3402	-28.0

Table S3. Calculated hydrogen bond distances ($d_{X\cdots H}$, Å), charge on acidic proton and interaction energy (ΔE_{HB}, kJ/mol) of ethyl cyanoacetate and acetophenone with the solvents.

	Ethyl cyano acetate			Acetophenone		
Solvent	$d_{x\cdots H}$	Charge on acidic proton	ΔE_{HB}	$d_{x\cdots H}$	Charge on acidic proton	ΔE_{HB}
Cyclohexane	2.83	0.238	+0.9	--	--	--
Benzene	2.89	0.240	-0.8	--	--	--
1,2 dichloroethane	2.92	0.249	-8.8	*2.94	0.197	-0.2
Nitrobenzene	2.35	0.252	-11.3	2.54	0.220	-10.9
Benzonitrile	2.37	0.275	-19.4	2.62	0.209	-06.2
Dimethyl sulfoxide	2.06	0.292	-26.2	2.32	0.235	-16.3
Teriray butanol	2.24	0.263	-10.9	--	--	--
n-butanol	2.22	0.260	-22.8	--	--	--
Isopropanol	2.20	0.259	-12.3	--	--	--
Water	2.29	0.258	-12.5	--	--	--

*For solvent Bromobenzene,

Table S4. Adsorption energy (kcal/mole) and bond distance (Å) between the 4T Zeolite models and solvents with different AN/ DN.

Solvent	**AN**	**DN**	$\mathbf{d_{x\cdots H}}$	$\mathbf{\Delta E_{HB}}$
Cyclohexane	0	0	2.10	+1.25
Benzene	8.6	0	2.30	-3.7
1,2 dichloroethane	16.7	0	2.40	-3.0
Nitrobenzene	14.8	4.4	1.76	-8.3
Benzonitrile	15.5	11.9	1.79	-9.9
Acetonitrile	18.9	14.1	1.80	-9.5
1,4-dioxane	10.3	14.3	1.66	-11.1
1,2-dimethoxyethane	10.2	20.0	1.63	-11.2
N, N-DMF	16	26.6	1.59	-16.0
Dimethyl sulfoxide	19.3	29.8	1.57	-18.5
Triethylamine	1.4	61	1.07	-61.0
Tertiary butanol	27.1	21.9	1.58	-13.6
Isopropyl alcohol	33.5	21.1	1.59	-14.1
1-butanol	36.8	19.5	1.59	-14.0
water	54.8	18.0	1.62	-14.0

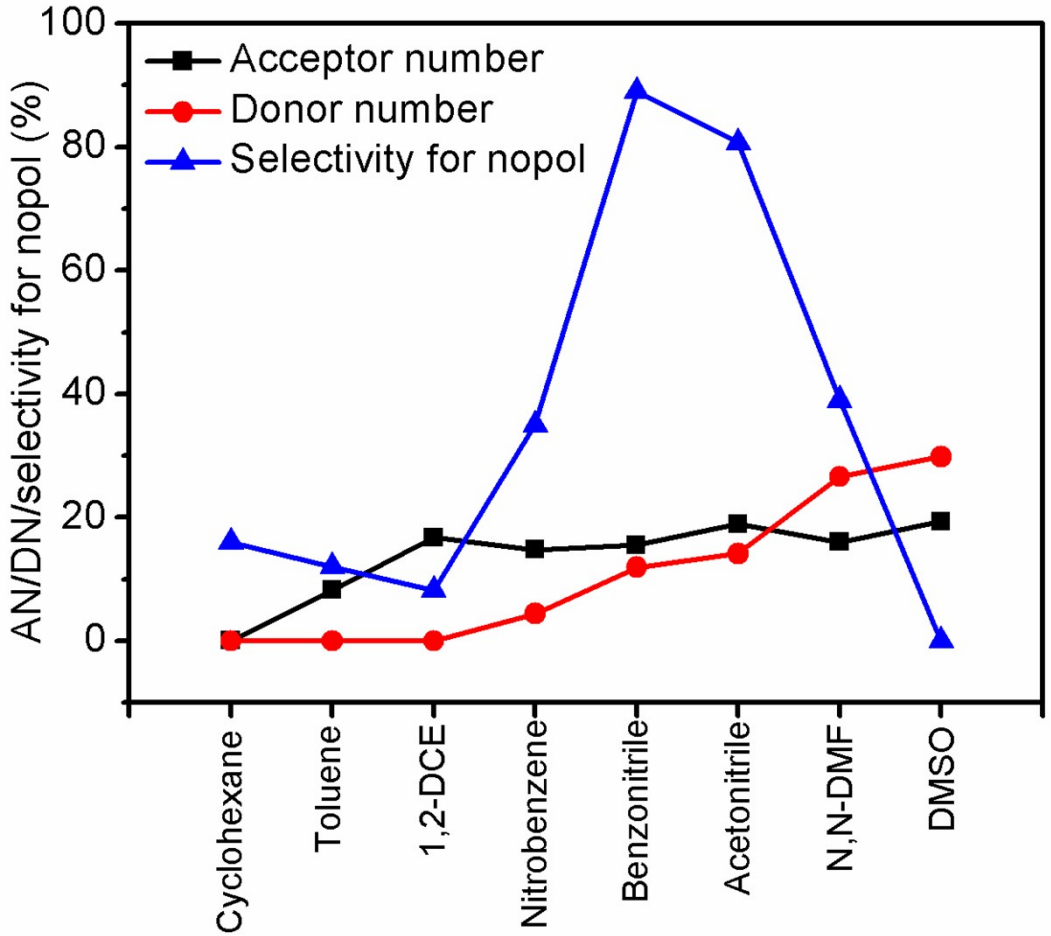

Figure S1. Plot of the nopol selectivity in Prins condensation reaction against solvents with different AN and DN. (The low selectivity for N,N-DMF and DMSO is due to the negligible conversion of β-pinene < 5%)

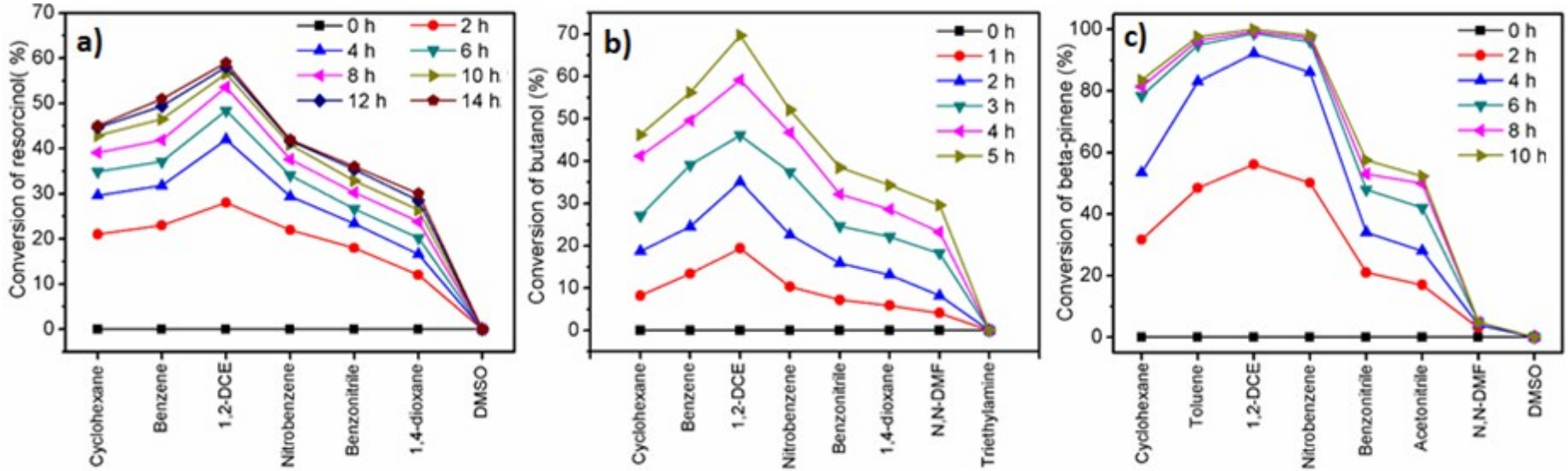

Figure S2. Plot the catalytic activity at different reaction times for solvents with different AN and DN in a) Friedel-Craft alkylation of resorcinol, b) butanol esterification and c) Prins condensation of β-pinene.

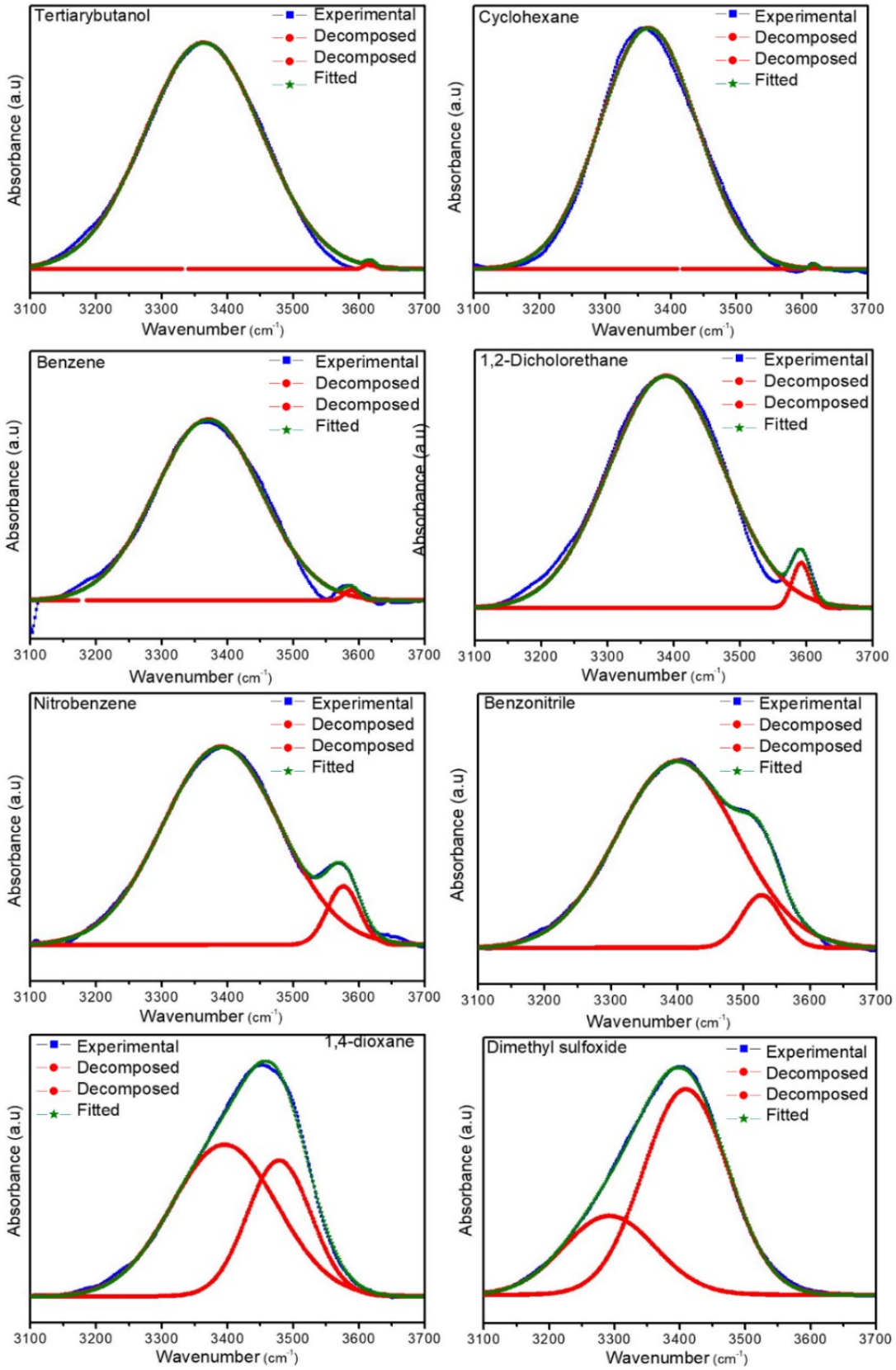

Figure S3. FT-IR spectra of TBA in the different solvents.

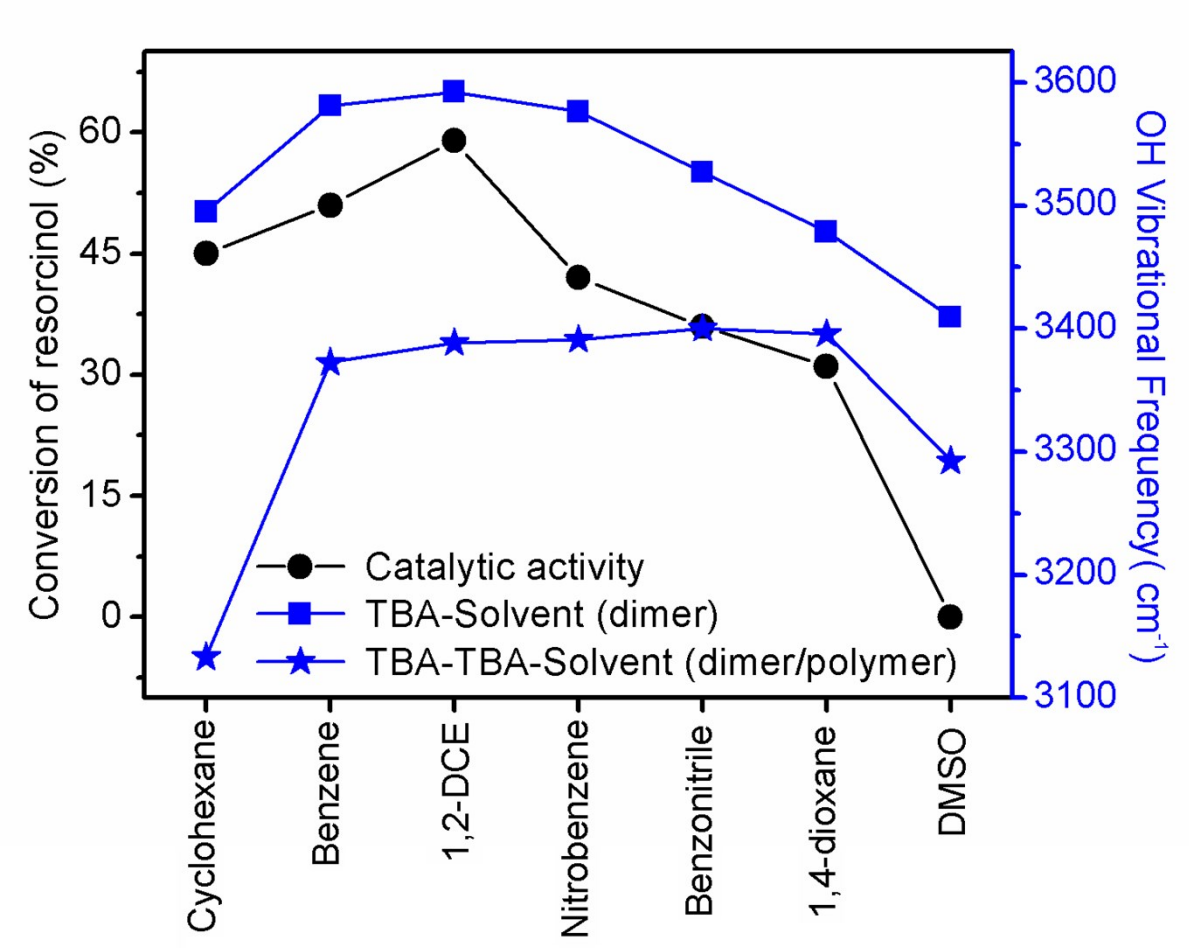

Figure S4. Plot of -OH vibrational frequency of TBA and resorcinol conversion in Friedal-Craft alkylation reaction for different mixtures TBA-Solvent (dimer) and TBA-TBA-Solvent (dimer/polymeric) .

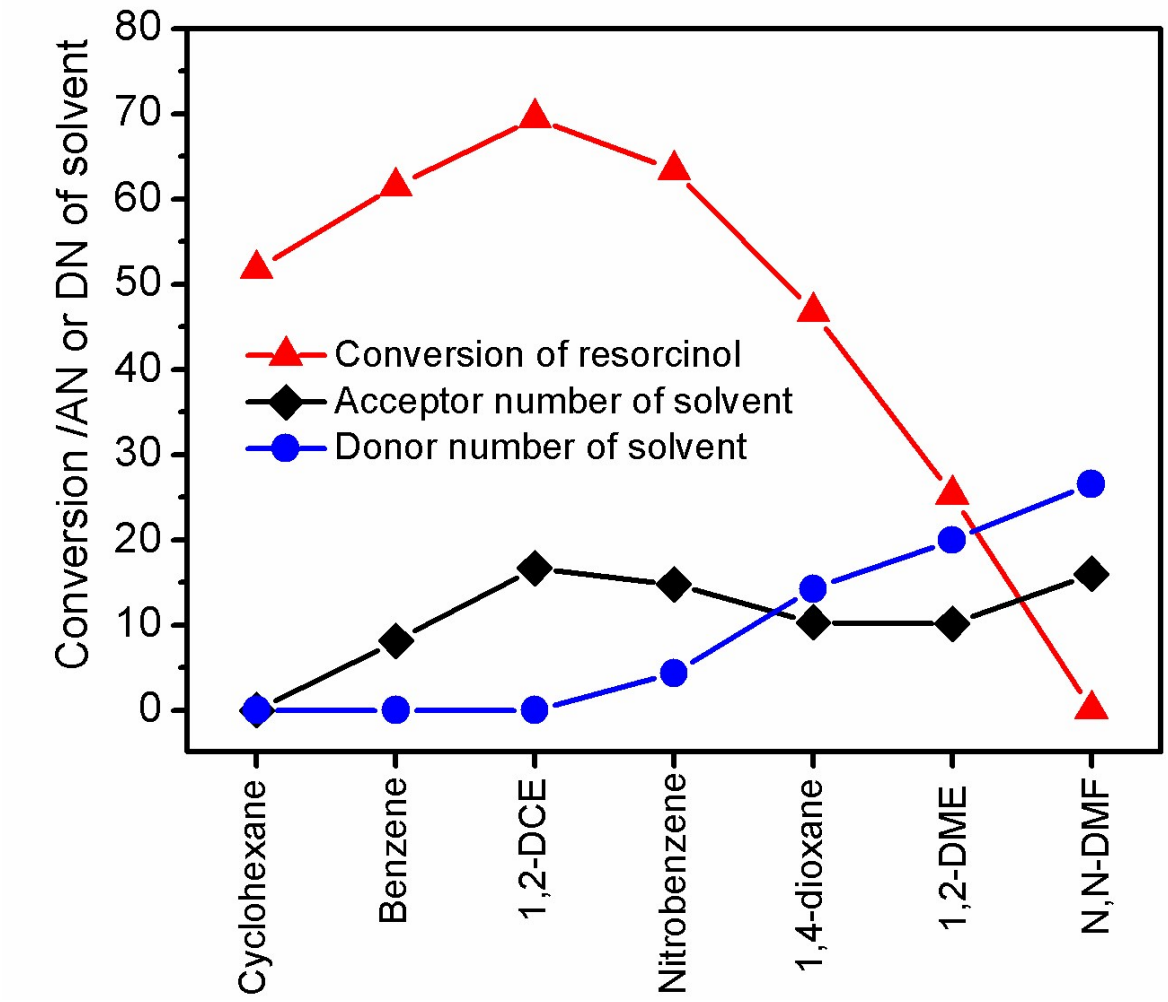

Figure S5. Catalytic activity in Friedel-Craft reaction using MTBE as alkylating agent over SZ catalyst versus the AN and DN of solvents.

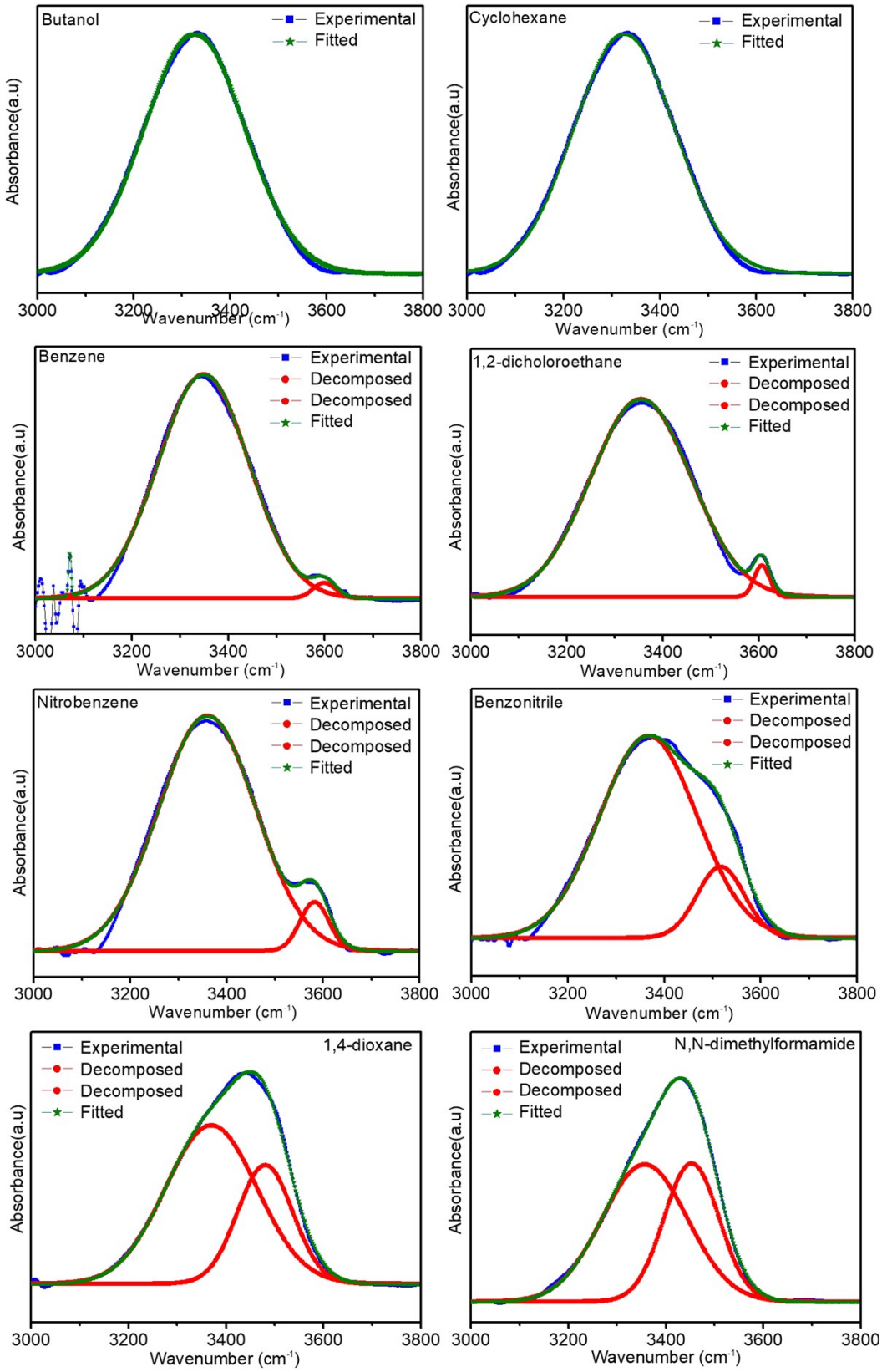

Figure S6. FT-IR spectra of n-butanol in the different solvents.

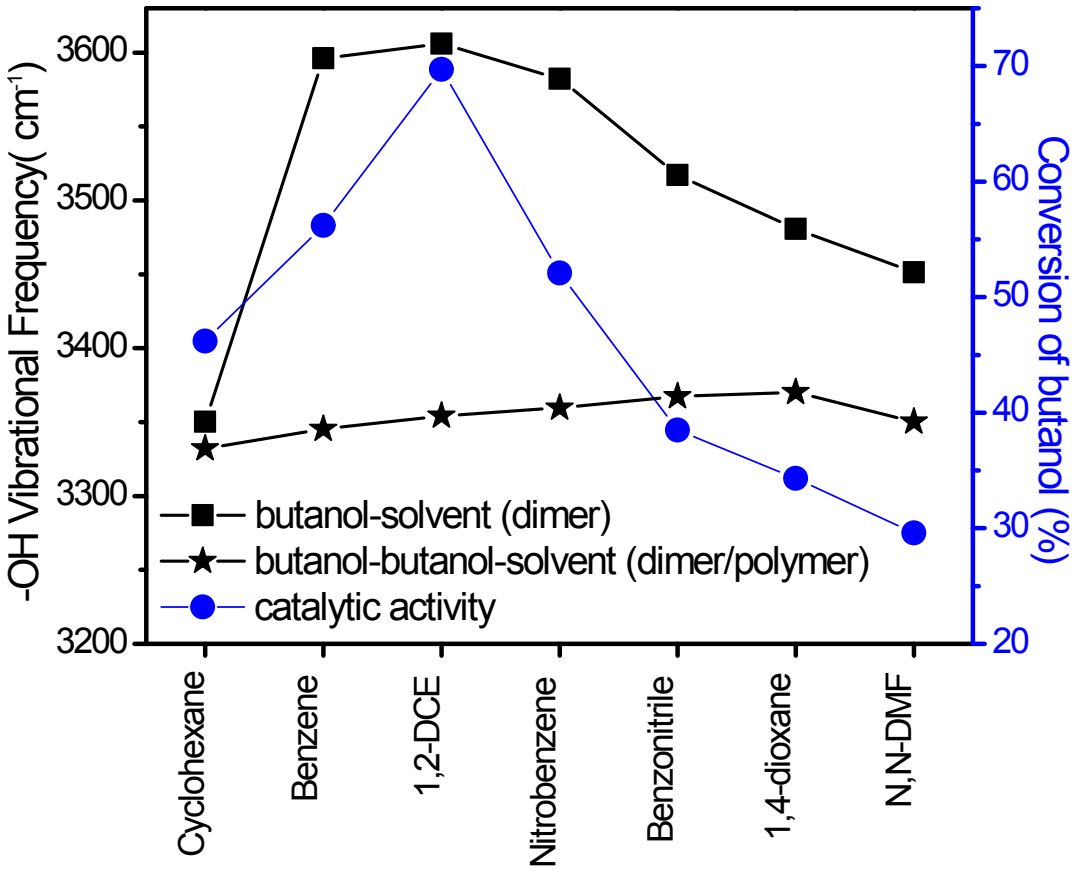

Figure S7. Plot of -OH vibrational frequency of butanol and resorcinol conversion in butanol esterification for different mixtures butanol-Solvent (dimer) and butanol-butanol-Solvent (dimer/polymeric).

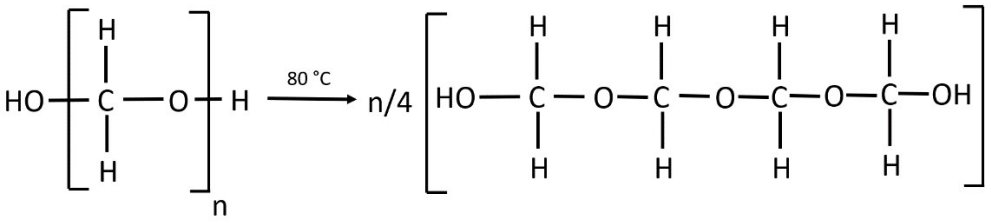

Figure S8. Plausible mechanism for the decomposition of PF to smaller PF units.

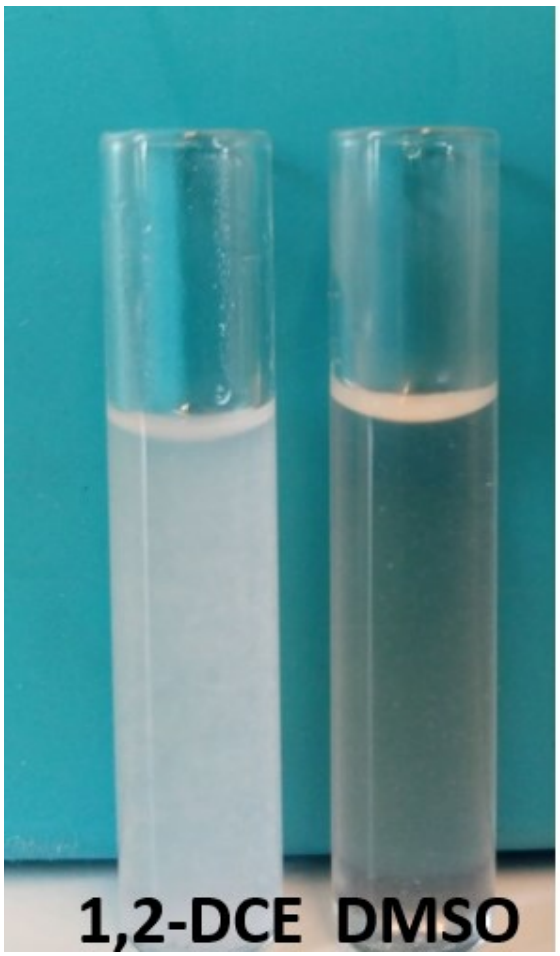

Figure S9. The picture presents the decomposition of PF at 80 °C in 1,2-DCE and DMSO. The solution is more cloudy in 1, 2-DCE and is clearer in DMSO.

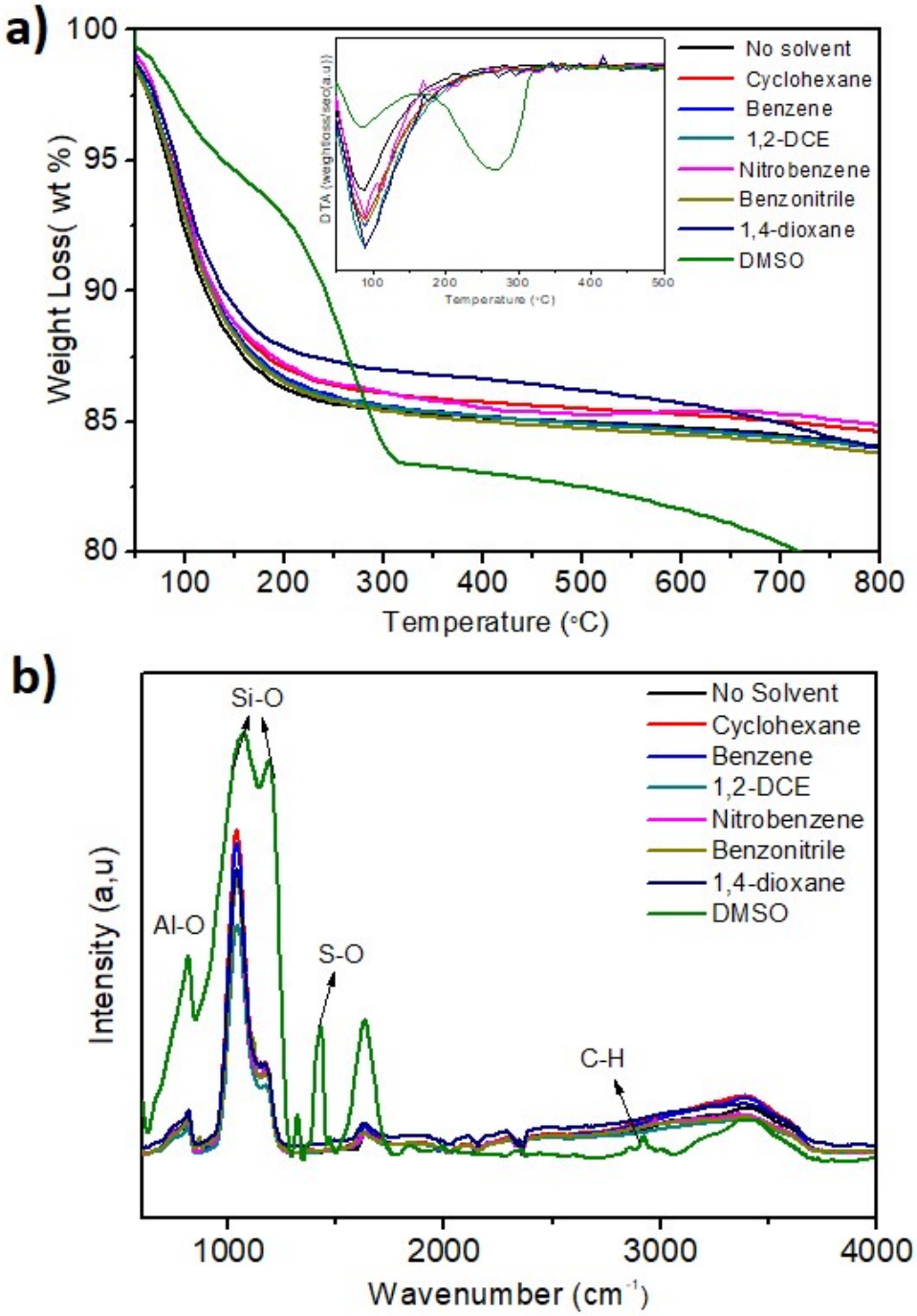

Figure S10. TG-DTA and FTIR spectra of HY zeolite after solvent adsorption.

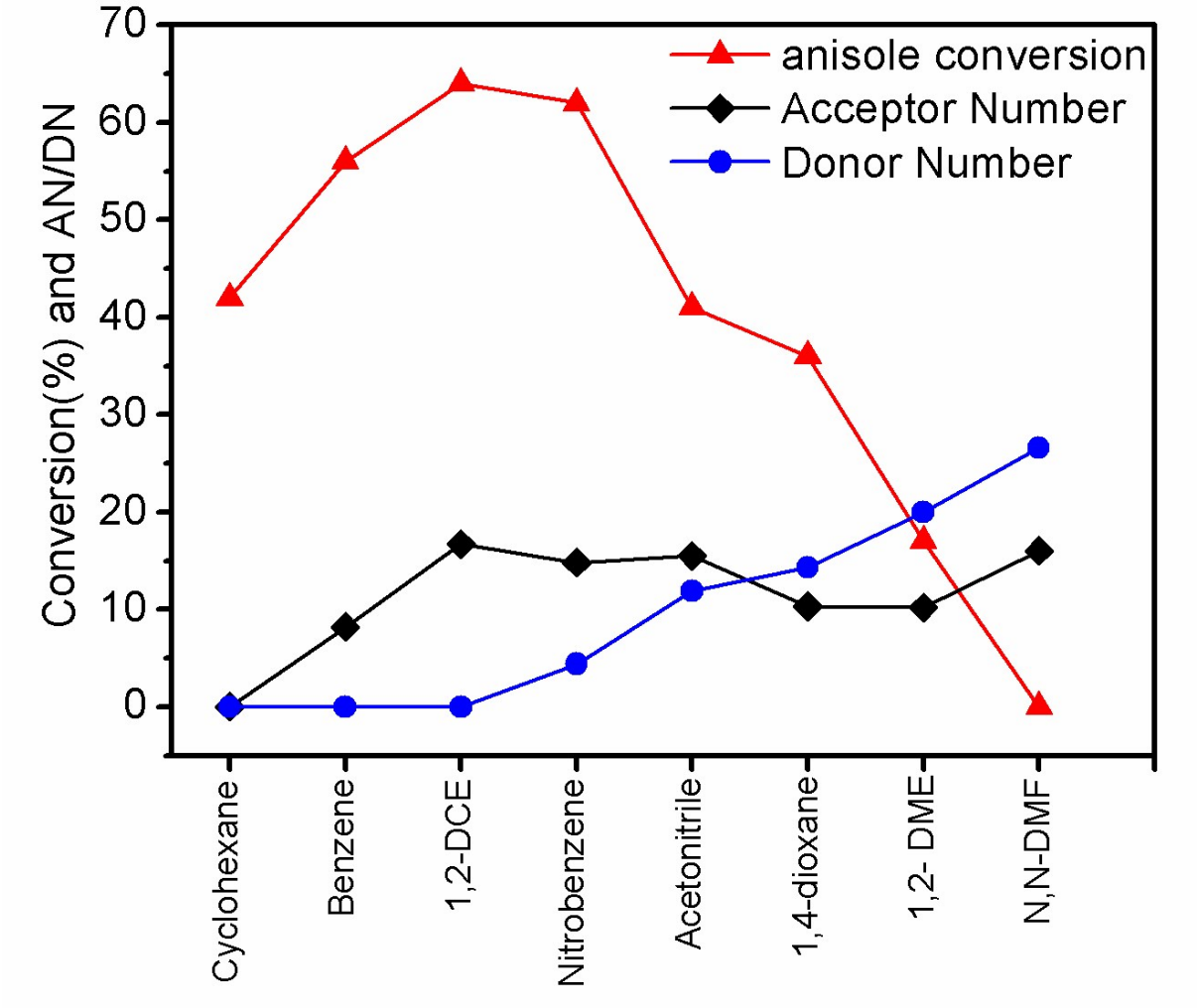

Figure S11. Plot of catalytic activity versus the AN and DN of solvents in acid catalyzed acylation of anisole. **(**Reaction conditions: Anisole =10 mmol g, acetic anhydride= 50 mmol, Solvent = 3 ml, Catalyst H-beta zeolite = 200 mg, Temperature = 80 °C, *o*-Xylene = 0.2 ml (internal standard), Reaction time= 4 h)

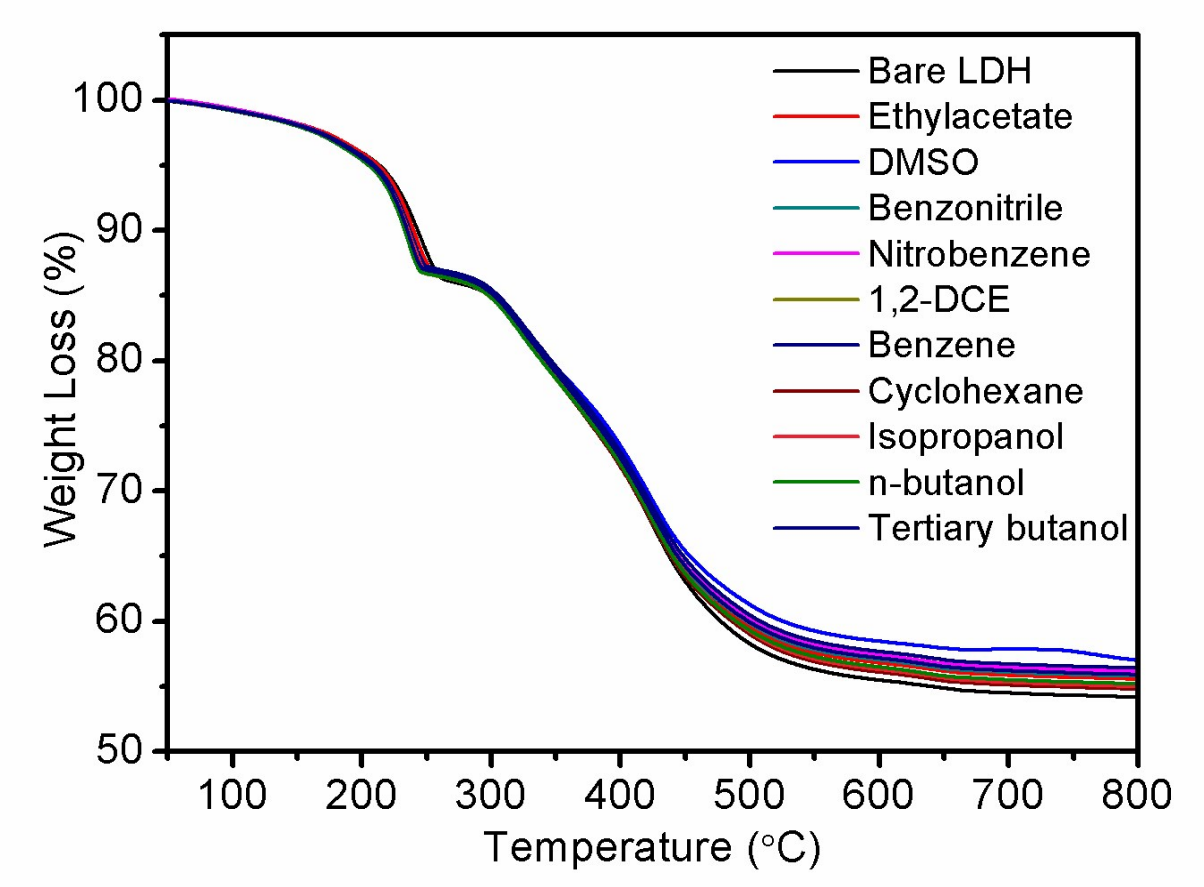

Figure S12. TGA analysis of hydrotalcite after solvent adsorption.

References

1. Marakatti, V. S.; Shanbhag, G. V.; Halgeri, A. B., Sulfated zirconia; an efficient and reusable acid catalyst for the selective synthesis of 4-phenyl-1,3-dioxane by Prins cyclization of styrene. *Applied Catalysis A: General* **2013,** *451*, 71-78.
2. Marakatti, V. S.; Halgeri, A. B.; Shanbhag, G. V., Metal ion-exchanged zeolites as solid acid catalysts for the green synthesis of nopol from Prins reaction. *Catalysis Science & Technology* **2014,** *4* (11), 4065-4074.
3. Marakatti, V. S.; Marappa, S.; Gaigneaux, E. M., Sulfated zirconia: an efficient catalyst for the Friedel–Crafts monoalkylation of resorcinol with methyl tertiary butyl ether to 4-tertiary butylresorcinol. *New Journal of Chemistry* **2019,** *43* (20), 7733-7742.
4. Boys, S. F.; Bernardi, F., The calculation of small molecular interactions by the differences of separate total energies. Some procedures with reduced errors. *Molecular Physics* **1970,** *19* (4), 553-566.
5. Hrouda, V.; Florian, J.; Hobza, P., Structure, energetics, and harmonic vibrational spectra of the adenine-thymine and adenine*-thymine* base pairs: gradient nonempirical and semiempirical study. *The Journal of Physical Chemistry* **1993,** *97* (8), 1542-1557.
6. Reina, M.; Martinez, A.; Cammarano, C.; Leroi, C.; Hulea, V.; Mineva, T., Conversion of Methyl Mercaptan to Hydrocarbons over H-ZSM-5 Zeolite: DFT/BOMD Study. *ACS Omega* **2017,** *2* (8), 4647-4656.
7. Kresse, G.; Hafner, J., Ab initio molecular dynamics for liquid metals. *Physical Review B* **1993,** *47* (1), 558-561.
8. Kresse, G.; Furthmüller, J., Efficiency of ab-initio total energy calculations for metals and semiconductors using a plane-wave basis set. *Computational Materials Science* **1996,** *6* (1), 15-50.
9. Kresse, G.; Joubert, D., From ultrasoft pseudopotentials to the projector augmented-wave method. *Physical Review B* **1999,** *59* (3), 1758-1775.
10. Perdew, J. P.; Burke, K.; Ernzerhof, M., Generalized Gradient Approximation Made Simple. *Physical Review Letters* **1996,** *77* (18), 3865-3868.
11. Grimme, S.; Antony, J.; Ehrlich, S.; Krieg, H., A consistent and accurate ab initio parametrization of density functional dispersion correction (DFT-D) for the 94 elements H-Pu. *The Journal of Chemical Physics* **2010,** *132* (15), 154104.
12. Grimme, S.; Ehrlich, S.; Goerigk, L., Effect of the damping function in dispersion corrected density functional theory. *Journal of Computational Chemistry* **2011,** *32* (7), 1456-1465.
13. Dědeček, J.; Tabor, E.; Sklenak, S., Tuning the Aluminum Distribution in Zeolites to Increase their Performance in Acid-Catalyzed Reactions. *ChemSusChem* **2019,** *12* (3), 556-576.
14. Pezzotta, C.; Fleury, G.; Soetens, M.; Van der Perre, S.; Denayer, J. F. M.; Riant, O.; Gaigneaux, E. M., Improving the selectivity to 4-tert-butylresorcinol by adjusting the surface chemistry of heteropolyacid-based alkylation catalysts. *Journal of Catalysis* **2018,** *359*, 198-211.
15. Kasinathan, P.; Lang, C.; Radhakrishnan, S.; Schnee, J.; D'Haese, C.; Breynaert, E.; Martens, J. A.; Gaigneaux, E. M.; Jonas, A. M.; Fernandes, A. E., "Click" Silica-Supported Sulfonic Acid Catalysts with Variable Acid Strength and Surface Polarity. *Chemistry – A European Journal* **2019,** *25* (27), 6753-6762.